Theoretical Study of the Interaction of the Ti Atom with CO_2: Cleavage of the C−O Bond

Imre Pápai*

Institute of Isotopes of the Hungarian Academy of Sciences, Spectroscopy Department, H-1525 Budapest, P.O.B. 77, Hungary

Joëlle Mascetti

Laboratoire de Spectroscopie Moléculaire et Cristalline, Université de Bordeaux I, 351, cours de la Libération, 33405 Talence Cedex, France

René Fournier

York University, Chemistry Department, North York, 4700 Keele Street, M3J 1P3 Canada

Received: January 30, 1997; In Final Form: April 3, 1997[⊗]

The interaction of s^2d^2 and s^1d^3 Ti atoms with the CO_2 molecule has been studied using density functional theory at the gradient-corrected level. The ground state Ti inserts with no energy barrier into a CO bond resulting in an OTiCO insertion product. The intrinsic reaction coordinate for the insertion process has been defined and the reaction mechanism has been investigated by analyzing various structures along this path. The singlet and triplet states of the final product are very close in energy. The comparison of the predicted vibrational frequencies and isotopic shifts for both states with those from matrix isolation infrared data reveals that the insertion product formed in low-temperature argon matrix corresponds to singlet state OTiCO. $Ti(CO_2)$ complexes in various coordination modes have also been located on the triplet and quintet potential energy surfaces, from which the triplet state (O,O) coordination mode is the most stable one lying, however, about 30 kcal/mol above the OTiCO molecule.

I. Introduction

Under normal conditions, carbon dioxide is one of the most stable triatomic molecules, and therefore its activation and conversion into useful organic compounds requires a huge amount of input energy. This energy, however, can be substantially reduced by using transition metal complexes as catalysts.[1] One possible route in understanding the mechanism of these catalytic processes is the investigation of reactions between transition metal atoms and CO_2. To this end, matrix isolation UV−visible and infrared spectroscopic experiments have been recently carried out for a series of first-row transition metal/CO_2 systems.[2] It has been found that the late transition metal atoms (Fe, Co, Ni, and Cu) formed one-to-one complexes ($M(CO_2)$) with CO_2, while those from the left-hand side in the periodic table (Ti, V, and Cr) inserted spontaneously into a CO bond yielding oxo−metal−carbonyl (O−M−CO) species. The OMCO insertion products were actually not observed in the experiments because they either decomposed into MO + CO or/and fixed another CO_2 molecule to form the $OM(CO_2)$ and $OMCO(CO_2)$ species.

Very similar results have been observed in matrix isolation studies of the M + H_2O reaction,[3,4] namely, metal atoms from Cr to Zn (except for Ni) formed $M(H_2O)$ adducts with water,[3] whereas reactions for the first three members of the series (Sc, Ti, and V)[4] and for Ni[5] yielded H−M−OH insertion products. The unique reactivity of Ni among the right-hand side transition metals has been attributed to the presence of low-lying ^{1}D state Ni atoms.[6]

Theoretical investigations of the interaction of second-row transition metal atoms with several small molecules (H_2O, NH_3, and CH_4)[7] have also shown significant differences in the binding mechanisms for the early and late transition metals.

Although several M + CO_2 systems have been investigated with various theoretical approaches,[8−13] none of them addressed the question of metal insertion. The present theoretical study focuses on the Ti + CO_2 → OTiCO reaction and it is aimed at understanding the reaction, mechanism and the driving forces in the insertion process. Our recent work on the Ni + CO_2 system[14] offers an opportunity to compare two different transition metal atoms, one from the left and the other from the right side of the periodic table. The Ti + CO_2 reaction has recently been studied by another matrix isolation group[15] using laser-ablated Ti atoms, and one of the reaction products has been identified as the OTiCO molecule. The structure of this product and the nature of the bonding in it will also be discussed in our paper.

II. Computational Method

The calculations in the present work were carried out at the same level of theory as in our recent density functional theory (DFT) studies on different transition metal−ligand systems.[14,16] Namely, the BP86 functional (Becke's nonlocal exchange[17] and Perdew's gradient-corrected correlation[18] functionals) and the (63321/5211/41) (for Ti[19]) and (5211/411/1) (for C and O[20]) orbital basis sets were used within the LCGTO-DF formalism[21] as implemented in the deMon program.[22,23] The integration grid and other technical details of the calculations were described in ref 16.

Due to the near degeneracy of the ground state and low-lying excited states for some of the investigated systems, the virtual orbitals were allowed to mix into the occupied space in the self-consistent field (SCF) procedure by using fractional occupations for orbitals close to the Fermi level. This option was always switched on in the geometry optimizations and in the calculation of energy gradients needed for the normal coordinate analysis. The smear parameter, i.e. the orbital energy window for

[⊗] Abstract published in *Advance ACS Abstracts,* May 15, 1997.

S1089-5639(97)00379-4 CCC: $14.00

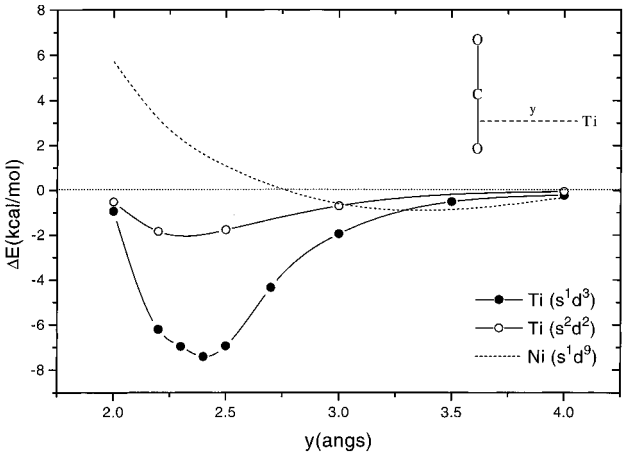

Figure 1. Interaction of s^2d^2 (^3F) and s^1d^3 (^5F) Ti and s^1d^9 (^3D) Ni atoms with a linear CO_2 molecule. The geometry of the CO_2 molecule is fixed at its equilibrium structure (R = 1.177 Å) and the distance between the midpoint of the CO bond and the metal atom is varied.

fractional occupation numbers, was always 0.3 eV. We took the usual (fixed occupation numbers) formula for the energy gradient, and this can introduce errors in the calculated properties.[24] However, test calculations on some of the molecules showed that the equilibrium geometries and the vibrational frequencies were not sensitive to the choice of the window size. Total energies, on the other hand, vary considerably with varying the smear parameter. Thus, in order to be consistent in the estimation of relative energies of the molecules, the total energies for the optimized structures were always recalculated without smearing, and the relative stabilities were determined from these values.

III. Results and Discussion

A. Interaction of Ti with Linear CO_2. As a very first step of our study, we derived two potential energy curves corresponding to the interaction of s^2d^2 (^3F) and s^1d^3 (^5F) Ti atoms with a linear CO_2 molecule as shown in Figure 1. For comparison, we have also depicted the curve for the Ni(s^1d^9)−CO_2 interaction obtained in our previous work.[14] Since the geometry of the CO_2 molecule was fixed at its equilibrium structure, only a part of the metal−ligand interaction energy is recovered in these calculations. Moreover, the curves presented in Figure 1 were derived with the smear option switched on and their shape turned out to be rather sensitive to the window size.[25] For this reason, these curves cannot describe accurately the long-range interactions; however, they may still provide a qualitative picture about the strength of the M−CO_2 interaction. For instance, we see a clear difference between the two metals: the Ni−CO_2 curve is essentially repulsive, while both Ti−CO_2 curves have well-defined minima with about 2 and 7 kcal/mol interaction energies for the triplet and quintet states, respectively.

The analysis of the Kohn−Sham orbitals of the Ti−CO_2 (linear) system shows that the metal−ligand binding is mostly due to the mixture of Ti 3d and CO_2 $3\pi^*$ orbitals. This orbital (see Figure 2) is singly occupied in both triplet and quintet states and it corresponds to a Ti → CO_2 charge transfer since the $3\pi^*$ orbital, which is a C−O antibonding combination of the p_π carbon and oxygen atomic orbitals, is unoccupied in free CO_2 and becomes partially occupied in the complex. Therefore, the Ti−CO_2 bond has a slight ionic character, which becomes more important when the complex is allowed to relax, as we will see later on. The other component of the Ti−CO_2 interaction is the repulsive interaction between the Ti 4s and the occupied CO_2 σ orbitals, which is usually reduced by the hybridization

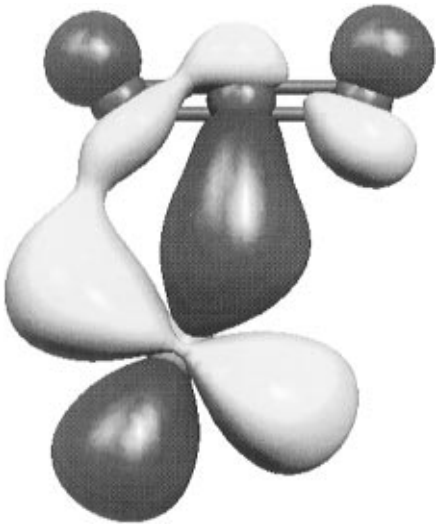

Figure 2. The 3d−$3\pi^*$ bonding orbital of the Ti + CO_2 (linear) system. (Plotted with the Molekel visualization program.[26])

of the metal 4s and $3d_\sigma$ orbitals. The reason the Ti−CO_2 interaction in the present geometrical arrangement is favorable for the quintet state is that the σ-repulsion is stronger for the s^2d^2 configuration than for s^1d^3. As for the difference in the nature of the Ni−CO_2 and Ti−CO_2 curves, we can point out two trends in the atomic properties of the transition metal series both indicating that the 3d−$3\pi^*$ bonding interaction becomes less dominant for the late transition metals. The first is the strong contraction of the 3d orbitals with respect to the 4s as the atomic number increases, and the second is the increase of ionization potential of metal atoms along the row. For the two metal atoms in question, for example, the $sd^n \rightarrow sd^{n-1}$ ionization potentials are quite different: they are 6.0 (Ti) and 8.7 (Ni) eV.[27]

As a next step, we carried out geometry optimizations from various initial geometries (including linear and distorted CO_2 structures) on the triplet and quintet potential energy surfaces, and we found that the optimization procedure yielded either a Ti(CO_2) complex or an OTiCO molecule. The results for these two types of molecules will be discussed separately in the next two sections.

B. Ti(CO_2) Complex. Four stationary points have been located on the quintet potential energy surface of Ti(CO_2) corresponding to the four possible coordination modes of CO_2, i.e. (O,O)− ($\eta^2_{O,O}$), side-on (η^2_{CO}), C− (η^1_C), and end-on (η^1_O) coordination modes, which are all depicted in Figure 3. For the triplet state, only two of the four modes ($\eta^2_{O,O}$ and η^1_O) have been located; the optimization with initial side-on and C−coordination structures always led to spontaneous insertion of Ti atom into the C−O bond yielding the OTiCO product. Interestingly, no Ti(CO_2) complexes have been observed in matrix experiments whatever the production mode of Ti atoms was: thermal vaporization[2] or laser ablation.[15]

The equilibrium geometries of all six Ti(CO_2) isomers are given in Table 1 along with their relative stabilities. It is seen that the triplet state (O,O) coordination mode ($\eta^2_{O,O}$-tri) is the most stable isomer, and it is separated by at least 14 kcal/mol from all the others. This isomer is followed by the four quintet state forms, from which the first three (η^2_{CO}, η^1_C, and $\eta^2_{O,O}$) are rather close in energy (within 4 kcal/mol). The η^1_O-tri structure is the least stable form lying about 42 kcal/mol above the $\eta^2_{O,O}$-tri isomer. Table 1 also shows that we cannot establish a clear correspondance between the stability of the Ti(CO_2) complexes and the degree of distorsion of the CO_2 ligand upon coordination. Of the six isomers, the CO_2 molecule is most

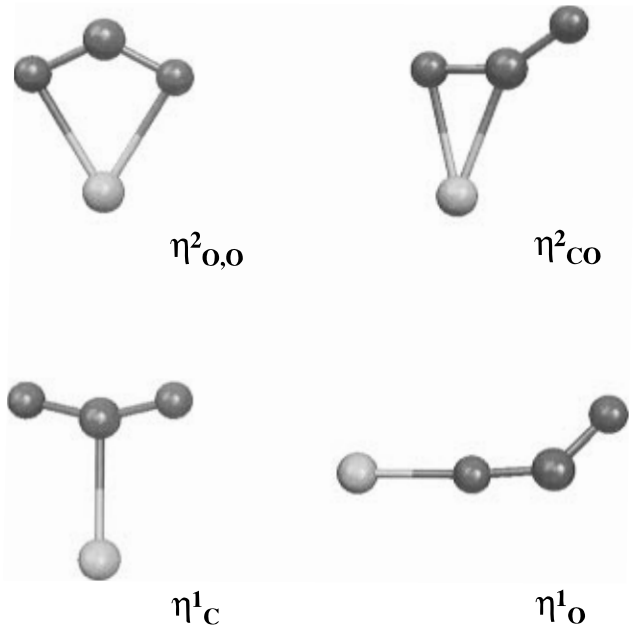

Figure 3. Various $Ti(CO_2)$ isomers located on the quintet potential energy surface. $\eta^2_{O,O}$, η^2_{CO}, η^1_C, and η^1_O denote (O,O), side-on C, and end-on coordination modes.

TABLE 1: Equilibrium Geometries and Relative Energies for Various Forms of the $Ti(CO_2)$ Complex (Bond Distances in angstroms, Angles in degrees, and Energies in kcal/mol)

	$\eta^2_{O,O}$-tri[a]	η^2_{CO}-qui	η^1_C-qui	$\eta^2_{O,O}$-qui	η^1_O-qui	η^1_O-tri
R(TiO)	1.890	2.093		2.173	1.936	2.147
R(TiC)		2.211	2.238			
R(C−O)[b]	1.354	1.267	1.220	1.261	1.272	1.189
R(C═O)	1.354	1.204	1.220	1.261	1.204	1.173
α(OCO)	112	145	153	126	139	179
α(TiOC)					169	171
Δ*E*[c]	0.0	+14.5	+16.9	+18.3	+26.8	+41.9

[a] "Tri" and "qui" refer to triplet and quintet spin states. [b] The equilibrium C−O bond length in free CO_2 is calculated to be 1.177 Å. [c] Relative energies with respect to the most stable species ($\eta^2_{O,O}$-tri) as obtained from direct comparison of calculated total energies. The true splitting of the triplet and quintet states is more considerable (see text).

distorted in $\eta^2_{O,O}$-tri and least distorted in η^1_O-tri but, in the remaining four isomers, the OCO angles and CO bond lengths do not follow the stability order. The sole isomer where the CO_2 molecule remains linear is η^1_O-tri, in which only the CO bond adjacent to the Ti atom is slightly lengthened, indicating a weak metal−ligand interaction. It is interesting to mention that the geometry of the CO_2 molecule in the ground state $Ti(CO_2)$ complex (R(CO) = 1.35 Å and α (OCO) = 112°) is very close to that found at a similar level of theory (BP86/TZP) for the ground state of the $Sc(CO_2)$ complex (R(CO) = 1.36 Å and α(OCO) = 112°; $^2A_1$ in $\eta^2_{O,O}$ coordination).[13]

The normal coordinate analysis carried out for the four most stable isomers indicated that the η^1_C-qui form is a transition state on the quintet potential energy surface with an imaginary frequency corresponding to the $\eta^1_C \rightarrow \eta^2_{CO}$ transition. The predicted IR spectra for the $\eta^2_{O,O}$-tri, η^2_{CO}-qui, and $\eta^2_{O,O}$-qui isomers are given in Table 2. We see that the two CO stretching frequencies in $\eta^2_{O,O}$-tri are extremely low and they fall quite close to each other, just as for the $^2A_1$ state of the $Sc(CO_2)$ complex.[13] In fact, no $M(CO_2)$ complexes with such low CO stretching frequencies have been observed yet. These frequencies lie much higher in the case of $\eta^2_{O,O}$-qui, and there is also a significant difference in the symmetric TiO stretching frequencies for the two states: it is about 150 cm^{-1} larger in $\eta^2_{O,O}$-tri. All these are consistent with a stronger metal−ligand interaction

TABLE 2: Calculated Harmonic Frequencies (in cm^{-1}) and IR Intensities (in Parentheses, in km/mol) for the Three Most Stable Forms of $Ti(CO_2)$

$\eta^2_{O,O}$-tri	$\eta^2_{O,O}$-qui	η^2_{CO}-qui
1008 (73) CO str (a_1)[a]	1547 (289) CO str (b_2)	1902 (349) C═O str (a′)
937 (271) CO str (b_2)	1281 (5) CO str (a_1)	1133 (168) C−O str (a′)
699 (2) OCO bend (a_1)	711 (3) OCO bend (a_1)	658 (137) OCO bend (a′)
507 (34) TiO str (a_1)	342 (47) TiO str (a_1)	398 (0) oop (a″)
390 (6) oop (a_1)	306 (12) oop (a_1)	364 (1) Ti−CO_2 str (a′)[b]
235 (54) TiO str (b_2)	257 (2) TiO str (b_2)	200 (6) Ti−CO_2 str (a′)

[a] Notation: str = stretching, bend = in-plane bending, oop = out-of-plane bending. [b] Both Ti−CO_2 str modes are mixtures of TiO str and TiC str vibrations, the first (364 cm^{-1}) being the in-phase, the other (200 cm^{-1}) the out-of-phase combination.

in the ground state complex, which is born out by the difference in the TiO and CO bond orders as well (they are M(TiO) = 0.93 and M(CO) = 1.28 in $\eta^2_{O,O}$-tri, and M(TiO) = 0.44 and M(CO) = 1.63 in $\eta^2_{O,O}$-qui). Table 2 also shows that the OCO bending frequency is not sensitive to the coordination mode, because it varies only in a rather narrow range (660−710 cm^{-1}) for the three forms presented in the table. The splitting of the two CO stretching frequencies is significantly larger in the η^2_{CO}-qui form, which follows from the fact that only one of the O atoms is involved in the metal−ligand bond. The frequencies of the CO_2 internal modes of this form are close to those obtained for the same coordination mode of $Ni(CO_2)$,[14] which is not really surprising in view of the similarity in the geometry of the CO_2 ligand in side-on $Ti(CO_2)$ and $Ni(CO_2)$ complexes (the OCO angle is 145° for both complexes and the corresponding CO bond distances are about the same as well). The metal−ligand frequencies, however, are calculated to be much higher for the $Ni(CO_2)$ complex.

The CO_2 binding energy in the most stable $Ti(CO_2)$ isomer relative to the ground state species ($Ti(s^2d^2) + CO_2$ ($^1\Sigma_g^+$)) at infinite separation is calculated to be D_0 = 34.9 kcal/mol, which would probably be lowered by about 4−5 kcal/mol if the correction for the basis set superposition error was included. The quintet states of $Ti(CO_2)$ are far less stable, since already the most stable quintet isomer (η^2_{CO}-qui) is bound only by 13 kcal/mol with respect to its dissociation asymptote ($Ti(s^1d^3) + CO_2(^1\Sigma_g^+)$). Considering that the experimental $s^2d^2 \rightarrow s^1d^3$ excitation energy of the Ti atom is about 16 kcal/mol,[27] the quintet states are in fact unbound relative to the ground state species.[28]

We mention here that these results sharply contradict those from a Hartree−Fock (HF) study,[10] which is actually the only theoretical work reported so far for $Ti(CO_2)$. The author of this study examined the CO_2 coordination toward Ti in all four possible arrangements and found the η^1_O-qui form to be the most stable one, followed by $\eta^2_{O,O}$-qui and η^2_{CO}-qui. The binding energies for these forms were calculated to be 26, 19, and 5 kcal/mol, respectively, relative to $Ti(s^2d^2) + CO_2(^1\Sigma_g^+)$. It is quite surprising to see a case where HF theory gives appreciable binding energies whereas DFT, which generaly provides upper bounds for binding energies, even at the nonlocal level, predicts the bond to be unstable. This contradiction can probably be related to the fact that the $Ti(s^1d^3) \rightarrow Ti^+(s^1d^2)$ ionization potential is underestimated by about 2 eV by HF theory (see Table 1 in ref 10), enhancing the ionic stabilization of the Ti−CO_2 bond, which may also alter the relative stabilities of different coordination modes. On the other hand, it appears that the present method underestimates the ionic contribution to the bonding, since the above ionization potential obtained in our calculations is about 1 eV too large compared to experiment, which means that the relative stabilities presented here should not be considered as very accurate predictions either. The clear

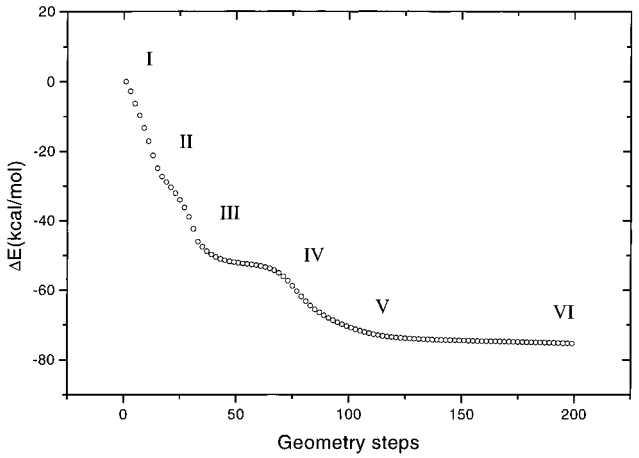

Figure 4. The variation of the total energy along the $Ti(s^2d^2) + CO_2$ $(^1\Sigma_g^+) \rightarrow OTiCO(^3A'')$ reaction path. The energies are given for each even number of geometry steps relative to the initial structure. Structures corresponding to steps numbered 0, 20, 40, 75, 100, and 200 will be referred to as structures I, II, ..., and VI.

separation of the $\eta^2_{O,O}$-tri isomer from the others, however, strongly suggests that this form is the lowest-lying $Ti(CO_2)$ isomer.

C. Ti + CO_2 → OTiCO Insertion. Geometry optimization for the interaction of the ground state Ti atom and CO_2 with initial η^2_{CO} and η^1_C structures resulted in the insertion of Ti into a C−O bond. It is quite remarkable that the insertion took place even with an undistorted CO_2 initial geometry, showing that the reaction for breaking the C−O bond has no energy barrier at all. In order to describe the mechanism of the insertion, we will follow the path that connects an arbitrarily chosen initial structure, namely, the one corresponding to the energy minimum of the $Ti(s^2d^2) + CO_2$ (linear) system (see Figure 1), to the global minimum of the triplet potential energy surface, which is equivalent to the triplet state of the OTiCO molecule. The minimization algorithm we used in the optimization is the steepest descent gradient method.[31] The largest average displacement parameter, which controls the magnitude of all the atomic displacements in the geometry optimization, has been chosen to be rather small (0.01 au) to ensure that the Born−Oppenheimer (BO) energy surface along the reaction path is mapped in detail, so that we can identify various characteristic stages in the insertion process. This way the optimization proceeds in small steps toward the final product, defining a path analogous to an intrinsic reaction coordinate.[32]

The variation of the total energy along the reaction path is depicted in Figure 4. Some characteristic structures (denoted by I, II, ..., VI) on the ΔE energy curve are illustrated in Figure 5. The evolution of various geometrical parameters along the reaction path is shown in Figure 6, whereas these parameters and some other calculated properties for structures I−VI are collected in Table 3.

Coming back to Figure 4, we point out first that the weakly bound Ti−CO_2 system (structure I) is very quickly stabilized as soon as the CO_2 molecule is allowed to relax. The stabilization energy of structure II is already about 30 kcal/mol with respect to structure I. The immediate bending of the ligand and the simultaneous lengthening of the C−O bonds indicate that a significant amount of negative charge is being transferred from the metal to CO_2. Indeed, from Table 3 we see that the Ti atom in structure II bears a positive charge equivalent to about 0.5 e^- charge transfer, which actually hardly changes for the rest of the reaction path. The region between the structures I and II can be viewed as a formation of a relatively strong Ti−C bond, since due to the diffuse lobe of the $3\pi^*$ orbital on the C atom, the charge transfer (i.e. the $3d(Ti)-3\pi^*(CO_2)$ overlap) takes place mainly through the carbon atom. That is

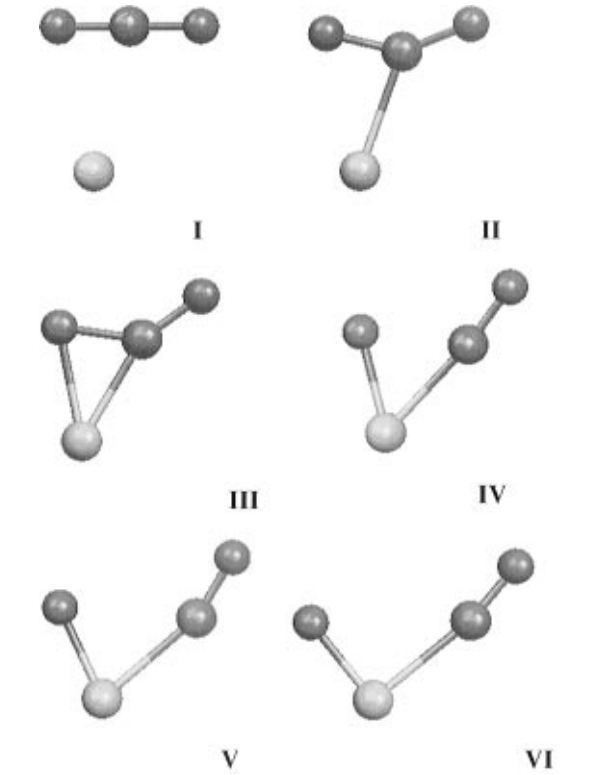

Figure 5. Structures obtained at step numbered 0, 20, 40, 75, 100, and 200 on the $Ti(s^2d^2) + CO_2(^1\Sigma_g^+) \rightarrow OTiCO(^3A'')$ energy curve.

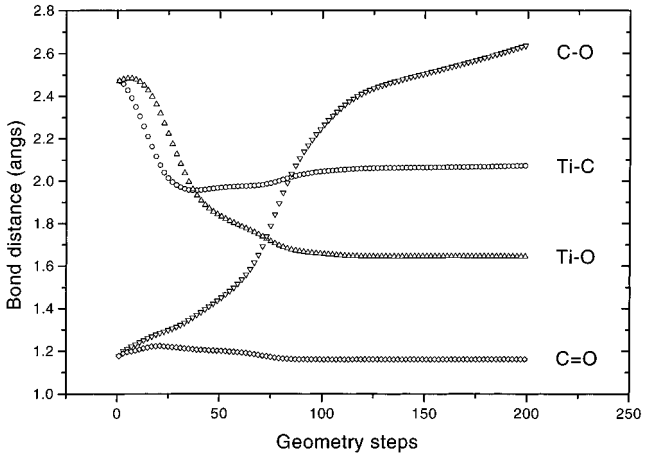

Figure 6. Bond lengths (in angstroms) as a function of geometry steps for the $Ti(s^2d^2)+CO_2$ $(^1\Sigma_g^+) \rightarrow OTiCO(^3A'')$ reaction.

TABLE 3: Calculated Properties for Structures I−VI

	I	II	III	IV	V	VI
R(TiC)[a]	2.47	2.10	1.96	1.99	2.05	2.07
R(TiO)	2.47	2.34	1.92	1.72	1.66	1.64
R(C−O)	1.18	1.28	1.37	1.79	2.25	2.64
R(C═O)	1.18	1.22	1.21	1.17	1.16	1.16
α(OCO)	180	145	136	119	116	130
ΔE[b]	0.0	−29.6	−50.3	−58.9	−70.7	−75.4
M(TiC)[c]	0.27	0.84	1.02	0.99	0.95	0.96
M(TiO)	0.16	0.50	1.03	1.79	2.14	2.24
M(C−O)	1.94	1.48	1.07	0.40	0.15	0.08
M(C═O)	2.13	1.91	2.01	2.23	2.32	2.33
Q(Ti)[d]	0.02	0.49	0.46	0.47	0.46	0.46

[a] Geometries (bond lengths in angstroms, angles in degrees). [b] Stabilization energies (in kcal/mol) with respect to structure I. [c] Mayer bond orders.[33] [d] Net positive charge on Ti atom.

why the Ti−C bond in structure II is shorter by more than 0.2 Å than Ti−O.

This latter bond is strengthened, however, in the next stage of the reaction, and the two bond distances and the corresponding bond orders (see Table 3) become about equal in structure III. Consequently, the C−O bond adjacent to Ti is further elongated, the C−O bond order gets close to 1, and at the same time the OCO angle is further decreased. Structure III therefore corresponds to the triplet state side-on Ti(CO_2) π-complex (η^2_{CO}-tri). In this complex, the 3d(Ti)−3π*(CO_2) orbital is doubly occupied, and therefore it is far more stable than the η^2_{CO}-qui complex, in which the above bonding orbital is singly occupied. Table 3 shows that the metastable η^2_{CO}-tri complex is stabilized by about 50 kcal/mol with respect to structure I, i.e. it lies well below the $\eta^2_{O,O}$-tri Ti(CO_2) isomer.

The ΔE energy curve becomes rather flat going from structure III to IV. Although the total energy of the system varies only by a few kcal/mol, this is the region where the C−O bond breaks up as seen from the shape of the C−O curve in Figure 6. The reason the system still stabilizes upon the cleavage of the C−O bond is that the Ti−O bond strengthens considerably: it shortens by 0.2 Å from structure III to IV and it has already double-bond character in structure IV. The other C−O bond distance at this point (1.17 Å) and also the corresponding bond order (2.23) are typical for a coordinated carbonyl group. It seems, therefore, that the energy gain obtained on the formation of the Ti═O and Ti−CO bonds in this step of the reaction exceeds the energy required to cleave the C−O bond of CO_2.

In the next stage, the energy decreases again to a greater extent. The stabilization of about 10 kcal/mol between structures IV and V is related to the opening of the OTiC angle and an additional strengthening of the Ti−O bond. The TiO bond length in structure V is quite close to that in the free TiO molecule (R_e = 1.62 Å[34]); therefore, it can be viewed as a TiO−carbonyl complex.

The calculated properties do not change much after structure V except the valence angles. These parameters slowly relax to about straight (TiCO) and right (OTiC) angles. Figure 6 indicates that the geometry optimization has not converged even at step number 200, owing to the flat potential energy surface, on which the final convergence of the steepest-descent algorithm is very slow. More sophisticated minimization algorithms would of course locate the minimum in a sufficiently small number of geometry steps. In the present work, the final geometry of the OTiCO molecule (and the equilibrium geometries for all the other systems) were determined by using the standard BFGS algorithm.[31] The geometry of the fully optimized OTiCO molecule is reported in the next section.

The above analysis suggests a reasonable reaction mechanism for the Ti insertion. In the first step of the reaction, a weakly bound collision complex of ground state Ti and CO_2 is formed followed by a quick relaxation of CO_2 occuring on the time scale of the OCO bend vibrational period. After the formation of a strongly bound η^2_{CO} complex the system "rolls" further downhill toward the global minimum, while the C−O bond is cleavaged and the strong Ti═O bond is formed. Finally, the OTiCO complex relaxes to its equilibrium structure. The kinetic bottleneck of the reaction is presumably the first step, where the CO_2 molecule either bounces away from Ti on a time scale shorther than one vibrational period or stays close over that time period, distorts, and the reaction proceeds toward the η^2_{CO} complex.

These results prompt us to conclude that the ground state Ti atom inserts spontaneously (i.e. with no energy barrier) into the C−O bond of the CO_2 molecule. This conclusion is fully in line with the findings of both matrix isolation IR studies[2,15] reported for the Ti/CO_2 system in that none of them found one-to-one Ti(CO_2) complexes among the reaction products but they both showed the formation of insertion products. Mascetti and Tranquille[2] showed that in neat CO_2 matrices, side-on coordination occurred on the OTiCO insertion species, leading to the formation of OTi(CO)(CO_2), whereas in argon dilute matrices, the OTi(CO_2) complex was formed. Indeed, our preliminary DFT calculations show that the interaction of a CO_2 molecule with OTiCO leads to the formation of a fairly stable OTi(CO)-(CO_2) complex ($D_e(CO_2)$ = 28 kcal/mol) in which CO_2 is side-on coordinated to Ti and the OTiCO and Ti(CO_2) units lie in perpendicular planes. Further calculations on various oxo−Ti-(CO_2) complexes are in progress.

TABLE 4: Equilibrium Geometries and Relative Energies for Various Spin States of OTiCO

	singlet	triplet	quintet
R(TiO)[a]	1.641	1.637	1.898
R(TiC)	1.979	2.086	2.021
R(CO)	1.186	1.163	1.175
α(OTiC)	102.5	97.0	117.4
α(TiCO)	179.7	175.9	167.9
ΔE[b]	+2.2	0.0	+67.9

[a] Bond lengths in angstroms, angles in degrees. All states have planar equilibrium structures. [b] Energies (in kcal/mol) relative to the most stable state (triplet).

Before we proceed to the characterization of the OTiCO molecule, we note that the reaction mechanism we described here is a simplified model, not only because it refers to a model system with infinitesimal kinetic energy but also because the intrinsic reaction path we defined is not unique and we assumed that the reaction proceeds on a single BO surface. For example, the smearing of the electrons around the Fermi level implies that some parts of the energy curve correspond to a path on a surface which is the average of two or more BO surfaces. This is actually the case only for the first piece of the ΔE curve between structure I and II since the occupied and virtual orbitals for both spins become sufficiently separated after structure II and the virtual orbitals are not mixed into the occupied space for the rest of the reaction path. Also, we should consider the possibility of surface crossings, which may occur for instance in the last stage of the reaction, where the structures and the energies of the singlet and triplet states of OTiCO are fairly similar (see next section). We add here that for the sake of completeness we have performed an optimization on the singlet state surface as well and found that, starting with a η^2_{CO} initial structure (similar to structure III), the optimization ended up with the insertion product, just as for the triplet case. Finally, we should not forget about the fact that the reaction path can show a variance with the choice of the exchange−correlation functional and the basis set. It cannot be ruled out, for instance, that one gets a barrier between the π-complex and the insertion product at a different level of theory. It would be surprising, however, to find an energy barrier higher than a few kcal/mol, so we do not expect to reach a different conclusion when using a different functional and a more extended basis set.

D. OTiCO Insertion Product. The equilibrium geometries and the relative stabilities of various spin states of the OTiCO molecule are compiled in Table 4. It is seen that the singlet and triplet states are very close in energy: the latter state is favored only by 2 kcal/mol. The quintet state, however, is well separated from them being almost 70 kcal/mol less stable. Not only the stabilities of the singlet ($^1A'$) and triplet ($^3A''$) states are similar but their structures show resemblance as well, at least, as far as their planarity and their OTiC and TiCO angles

TABLE 5: Calculated Harmonic Frequencies (in cm^{-1}) and IR Intensities (in km/mol) for the ^{1}A′ and ^{3}A″ States of OTiCO

	assignment	^{1}A′	^{3}A″	expt[a]
ω_1	CO str	1881 (618)	1986 (1139)	1867
ω_2	TiO str	967 (207)	991 (176)	953
ω_3	TiC str	495 (5)	398 (5)	
ω_4	TiCO bend	365 (4)	339 (6)	
ω_5	out-of-plane	326 (41)	241 (14)	
ω_6	OTiC bend	190 (17)	230 (3)	

[a] From ref 15.

TABLE 6: Calculated and Observed Isotopic Shifts (in cm^{-1}) for the CO Stretching and TiO Stretching Modes of OTiCO

	^{13}C			^{18}O		
	^{1}A′	^{3}A″	expt[a]	^{1}A′	^{3}A″	expt[a]
CO stretching	44.0	45.6	43.0	42.1	46.0	40.6
TiO stretching	0.0	0.0	0.0	41.0	42.4	40.9

[a] From ref 15.

are concerned. The Ti−O and Ti−C bonds appear to be stronger in the singlet state, as judged from their bond lengths. This is only partially supported by the predicted vibrational frequencies, which are shown in Table 5. The Ti−C bond is definitely stronger in the ^{1}A′ state, indicated by the notable difference in the TiC stretching and CO stretching frequencies, however, the TiO stretching frequency is slightly higher in the triplet case.

As we already mentioned before, the OTiCO molecule has recently been identified experimentally in a matrix isolation IR study.[15] Using the laser ablation technique, Chertihin and Andrews examined the reactions of laser-ablated Ti, TiO, and TiO_2 with CO on condensation with excess argon. They found that among other carbonyl products, a molecule characterized by two IR bands at 1867 and 953 cm^{-1} was always formed in these reactions. Similar experiments for the Ti + CO_2, Ti + $^{13}CO_2$, and Ti + $C^{18}O_2$ systems confirmed that this molecule is OTiCO and the above two bands correspond to CO stretching and TiO stretching vibrations. Given the almost equal stability of the ^{1}A′ and ^{3}A″ states of OTiCO, it is interesting to compare the observed frequencies with the values predicted for both states. The comparison (see Table 5) clearly shows a better agreement for the singlet state, in particular, the CO stretching frequency of the ^{3}A″ state seems fairly high, which is even more apparent if we consider that for free CO we calculate a frequency (2108 cm^{-1}) that is too low as compared to experiment.[35] We can also parallel the observed and theoretical isotopic shifts for the two observed modes. The comparison is presented in Table 6, and we again see a better agreement for the singlet state. It seems therefore likely that the species formed in the ablation experiments is the ^{1}A′ state OTiCO molecule.

In order to estimate the OTi−CO binding energy, we performed calculations for the TiO diatomic molecule. The calculated equilibrium properties of the ground state ($^3\Delta$) TiO are R_e = 1.627 Å, ω_e = 1026 cm^{-1}, and D_e = 160 kcal/mol,[36] which are all well in line with the experimental R_e = 1.620 Å, ω_e = 1009 cm^{-1}, and D_e = 158 kcal/mol values.[34] The OTi−CO binding energy is then obtained from the energy of the OTiCO(^{3}A″) → TiO($^3\Delta$) +CO($^1\Sigma^+$) reaction, which is calculated to be 23 kcal/mol. Taking into account that the BP86 functional tends to overestimate the M−CO binding energies by at least 10 kcal/mol,[37] the CO molecule is probably only weakly bound in OTiCO, which may explain the formation of the TiO and CO fragments besides the main products in the Ti/CO_2 matrix isolation experiments.[2] On the other hand, the dissociation of the ^{1}A′ state of OTiCO into singlet state fragments is energetically less favored, because the singlet states of TiO lie at least 25 kcal/mol above the $^3\Delta$ state, which may give a rationale for the formation of the singlet state OTiCO species in the ablation experiments.

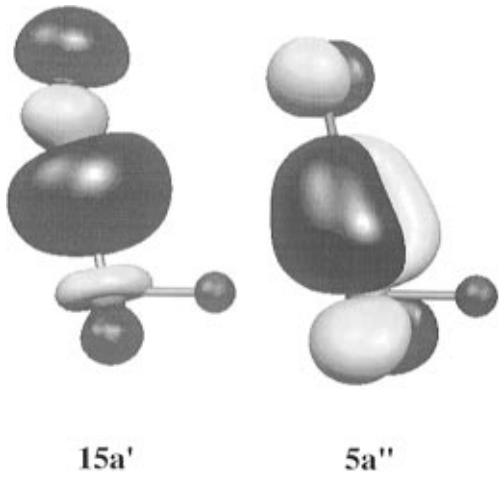

Figure 7. The 15a′ and 5a″ orbitals of the OTiCO molecule.

The electronic structure of the insertion product can be best described in terms of the orbitals of the TiO and CO constituents. The inspection of the Kohn−Sham orbitals reveals that most of the OTiCO orbitals have pure TiO or CO character; however, there are two orbitals (see Figure 7) having considerable contributions from both fragments. Assuming the OTiCO molecule to lie in the *xz* plane with the TiCO part along the *z* axis, the decompositions of the 15a′ and 5a″ orbitals (in ^{1}A′) are 79% CO(5σ) + 21% TiO($4s+3d_{zz}+4p_z$) and 66% TiO($3d_{yz}$) + 34% CO($2\pi^*$), respectively, where 5σ and $2\pi^*$ denote the carbon lone pair and the C−O π-antibonding CO orbitals, whereas 4s, $4p_z$, $3d_{zz}$, and $3d_{yz}$ are Ti atomic orbitals. The above decomposition suggests that the Ti−C bond arises from a CO → Ti σ-donation (15a′) and a simultaneous Ti → CO π-back-donation (5a″). This latter Ti−C bonding orbital is the highest occupied molecular orbital in the ^{1}A′ state and becomes singly occupied in ^{3}A″, resulting in the elongation of the Ti−C bond, lowering of the TiC str frequency, etc. The quasi-degeneracy of the ^{1}A′ and ^{3}A″ states suggests that the energy loss in exciting an electron from 5a″ to the lowest unoccupied molecular orbital (18a′ which is a ($4s+3d_{zz}+4p_z$) hybrid) and flipping its spin, is roughly compensated by the gain of the exchange energy. The 5a″ orbital is also responsible for the shape of the molecule, since the $3d_{yz}-2\pi^*$ interaction is optimal at a right OTiCO angle and at a planar arrangement of the two fragments. The deviation from 90° is probably associated with the repulsion of the filled CO and O π-orbitals in the molecular plane. Note that the $3d_{xz}$ orbital of the Ti atom does not contribute to the Ti−CO bond since it is involved in the bond formed with the O atom. Due to the difference in the electronegativities of Ti and O atoms, the Ti atom bears a net positive charge (+0.41) already in the free TiO molecule and it becomes even more positive in OTiCO (+0.48 in ^{3}A″ and +0.68 in ^{1}A′) since the OTi → CO charge flow is considerably larger than in the opposite direction.

IV. Concluding Remarks

Matrix isolation experiments have previously indicated that the formation of the OTiCO insertion product is easily obtained by the reaction of thermally evaporated[2] or laser-ablated[15] Ti atoms with CO_2. We have shown in this paper that the insertion of a ground state Ti atom into a CO bond of carbon dioxide takes place with no activation barrier and the OTiCO molecule

is thermodynamically far more stable than any of the possible $Ti(CO_2)$ complexes. We have proposed a plausible reaction mechanism for the insertion and described the structure of the insertion product.

Matrix isolation experiments have also shown that titanium oxides are reactive with CO_2 and a number of different oxidized species (TiO, TiO_2, $OTi(CO)(CO_2)$, $OTi(CO_2)$, O_2 $Ti(CO_2)$, etc.) have been detected in the experiments. Further experimental and theoretical studies are in progress to understand the formation of these molecules, which are of great interest as intermediates in catalytic reactions.

Acknowledgment. Financial supports from the Hungarian Academy of Sciences and CNRS are gratefully acknowledged. The support of the Hungarian Research Foundation (OTKA, Grant T020231) is also acknowledged.

References and Notes

(1) Braunstein, P.; Matt, D.; Nobel, D. *Chem. Rev.* **1988**, *88*, 747.
(2) Mascetti, J.; Tranquille, M. *J. Phys. Chem*. **1988**, *92*, 2177.
(3) Kauffman, J. W.; Hauge, R. H.; Margrave, J. L. *J. Phys. Chem*. **1985**, *89*, 3541.
(4) Kauffman, J. W.; Hauge, R. H.; Margrave, J. L. *J. Phys. Chem.* **1985**, *89*, 3547.
(5) Park, M.; Hauge, R. H.; Margrave, J. L. *High Temp. Sci.* **1988**, *25*, 1.
(6) Mitchell, S. A.; Blitz, M. A.; Siegbahn, P. E. M.; Svensson, M. *J. Chem. Phys.* **1994**, *100*, 423.
(7) Siegbahn, P. E. M.; Blomberg, M. R. A.; Svensson, M. *J. Chem. Phys*. **1993**, *97*, 2564.
(8) Caballol, R.; Marcos, E. S.; Barthelat, J. *J. Phys. Chem.* **1987**, *91*, 1328.
(9) Jeung, G. H. *Mol. Phys*. **1988**, *65*, 669.
(10) Jeung, G. H. *Mol. Phys*. **1989**, *67*, 747.
(11) Sirois, S.; Castro, M.; Salahub, D. R. *Int. J. Quantum Chem*. **1994**, *S28*, 645.
(12) Jeung, G. H. *Chem. Phys. Lett*. **1995**, *232*, 319.
(13) Sodupe, M.; Branchadell, V.; Oliva, A. *J. Phys. Chem*. **1995**, *99*, 8567.
(14) Galan, F.; Fouassier, M.; Tranquille, M.; Mascetti, J.; Pápai, I. *J. Phys. Chem*. **1997**, *101*, 2626.
(15) Chertihin, G. V.; Andrews, A. *J. Am. Chem. Soc*. **1995**, *117*, 1595.
(16) Pápai, I. *J. Chem. Phys*. **1995**, *103*, 1860.
(17) Becke, A. D. *Phys. Rev. A* **1988**, *38*, 3098.
(18) Perdew, J. P. *Phys. Rev. B* **1986**, *33*, 8822; erratum in *Phys. Rev. B* **1986**, *38*, 7406.
(19) Godbout, N.; Andzelm, J.; Salahub, D. R.; Wimmer, E. *Can. J. Chem*. **1992**, *70*, 560.
(20) Sim, F.; Salahub, D. R.; Chin, S.; Dupuis, M. *J. Chem. Phys*. **1991**, *95*, 4317.
(21) Salahub, D. R.; Fournier, R.; Mlynarski, P.; Pápai, I.; St-Amant, A.; Ushio, J. In *Density Functional Methods in Chemistry*; Labanowski, J., Andzelm, J., Eds.; Springer-Verlag: New York, 1991.
(22) St-Amant, A. Ph.D. Thesis, Université de Montréal, 1991.
(23) St-Amant, A.; Salahub, D. R. *Chem. Phys. Lett*. **1990**, *169*, 387.
(24) Warren, R. W.; Dunlap, B. I. *Chem. Phys. Lett*. **1996**, *262*, 384.
(25) The sensitivity of the shape of the energy curves shown in Figure 1 is not surprising since (1) for a given curve, the occupation numbers vary significantly as a function of metal−ligand distance (the d orbitals are degenerate at long distance and split up when approaching the CO_2 molecule); and (2) for a given metal−ligand distance, the occupation numbers vary with the window size.
(26) Flükiger, P. Ph.D. Thesis, University of Geneva, 1992.
(27) Martin, R. L.; Hay, P. J. *J. Chem. Phys*. **1981**, *75*, 4539.
(28) The present level of theory erroneously predicts the s^1d^3 (^{5}F) state of Ti to lie about 7 kcal/mol below the true ground state (s^2d^2 (^{3}F)). One way to obtain reliable adiabatic binding energies for cases where the complex correlates to an excited state metal atom is to calculate the binding energy with respect to the proper asymptotic limit and correct this value with the experimental atomic splitting. This procedure was found to be quite useful for several transition metal−ligand systems (see, for instance, refs 29 and 30).
(29) Fournier, F. *J. Chem. Phys*. **1993**, *99*, 1801.
(30) Ricca, A.; Bauschlicher, C. W. *J. Phys. Chem.* **1995**, *99*, 9003.
(31) Schlegel, H. B. In *Ab initio Methods in Quantum Chemistry − I*; Lawley, K. P., Ed.; Wiley: New York, 1987.
(32) Fukui, K. *Acc. Chem. Res*. **1981**, *14*, 363.
(33) Mayer, I. *Chem. Phys. Lett*. **1983**, *97*, 270.
(34) Huber, K. P.; Herzberg, G. *Molecular Spectra and Molecular Structure, Vol. IV., Constants of Diatomic Molecules*; Van Nostrand: Toronto, Canada, 1979.
(35) The frequency observed for the CO isolated in Ar matrix is 2138 cm^{-1}; see for instance: Dekock, R. L. *Inorg. Chem*. **1971**, *10*, 1205.
(36) D_e obtained from the energy of the $Ti(s^1d^3) + O(^3P) \rightarrow TiO(^3\Delta)$ reaction corrected with the experimental Ti atomic splitting (16 kcal/mol).
(37) Adamo, C.; Lelj, F. *J. Chem. Phys*. **1995**, *103*, 10605.